Structure and Dynamics of Li_3InBr_6 and $NaInBr_4$ by Means of Nuclear Magnetic Resonance*

Yasumasa Tomita, Koji Yamada, Hiroshi Ohki, and Tsutomu Okuda

Department of Chemistry, Faculty of Science, Hiroshima University, Kagamiyama, Higashi-Hiroshima 739-8526, Japan

Z. Naturforsch. **53a,** 466–472 (1998); received January 26, 1998

Li_3InBr_6 and $NaInBr_4$ have been synthesized and characterized by means of DTA, ^{81}Br NQR, ^{6}Li, ^{7}Li, ^{23}Na, and ^{115}In NMR, and AC conductivity. These measurements revealed the presence of phase transitions and cationic diffusion in both compounds. From the spin-lattice relaxation times of ^{81} Br NQR and the peak widths of ^{7}Li and ^{23}Na NMR spectra, it is deduced that the conduction is due to cationic diffusion. The activity energy for the Li^+ diffusion was found to be 24 kJ/mol for Li_3InBr_6.

Key words: NQR; NMR; Spin-lattice Relaxation Time; AC Conductivity; Cation Diffusion.

Introduction

We have already investigated the structure and dynamics of the compounds MBr-M′Br_3 (M = Li, Cu, Ag; M′ = Al, Ga) [1, 2]. In these compounds, the central metal M′ is tetrahedrally coordinated by Br^- ions. In some halocomplexes of In (III), however, M′ is octahedrally coordinated by halogen atoms. The difference in the In-halogen bonds of the tetrahedral and octahedral anions, and the factors which determine the shape of the anions are stereochemically interesting.

These complexes undergo phase transitions by cationic and anionic motions excited with increasing temperature. The electric conductivity changes abruptly at the temperature of the phase transition [3]. The relation between the ionic motions and the conductivity is also very interesting.

In the present study, we examined the bond nature, the anionic structure and the ionic motions in the In (III) halocomplexes by measuring ^{81}Br NQR, ^{6}Li, ^{7}Li, ^{23}Na, and ^{115}In NMR, and the electric conductivity.

Experimental

$NaInBr_4$ was obtained by heating an equimolar mixture of NaBr and $InBr_3$, sealed in a glass tube at 600 K. Li_3InBr_6 was prepared by mixing LiBr and $InBr_3$ in the molar ratio 3:1 and heating the mixture for two days at about 500 K. A single crystal was grown in a glass ampule by the Bridgman method.

DTA measurements were carried out, and powder X-ray diffraction patterns were recorded by a Rigaku Rad-B system, using CuK_α radiation. The diffraction data were analyzed by he Rietveld method, using a program developed by Izumi [4].

^{81}Br NQR signals were observed by a Matec pulsed spectrometer. The spin-lattice relaxation times T_1 were determined with the $90° - \tau - 90°$ pulse sequence. The error of the T_1 measurement was ca. ±10%.

^{6}Li, ^{7}Li, ^{23}Na, and ^{115}In NMR was observed by a Matec gating amplifier at 6.37 T with the Larmor frequencies of 39.92, 105.41, 71.75, and 59.41 MHz, respectively. The sample temperature was controlled within ±0.5 K.

Results and Discussion

Li_3InBr_6

Figure 1 shows the DTA curve for Li_3InBr_6. An endothermic peak appeared at 314 K on heating, and an exothermic one at 270 K on cooling. A rather large hysteresis was observed, indicating a first order phase transition.

We observed three ^{81}Br NQR lines of 59.292, 66.380, and 69.240 MHz at 77 K of Li_3InBr_6, suggesting the presence of three non-equivalent Br atoms. One resonance frequency is considerably lower than the other two. This suggests that the octahedron of the anion is considerably distorted. Figure 2 shows the temperature depen-

* Presented at the XIVth International Symposium on Nuclear Quadrupole Interactions, Pisa, Italy, July 20–25, 1997.

Reprint requests to Prof. T.Okuda; Fax 0824-24-0727.

0932-0784 / 98 / 0600-0466 $ 06.00 © – Verlag der Zeitschrift für Naturforschung, D-72027 Tübingen

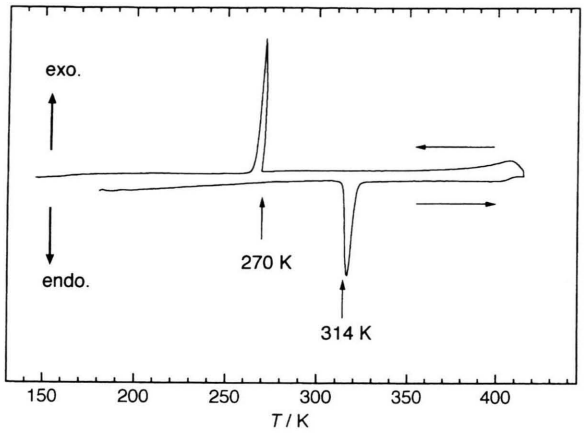

Fig. 1. DTA curve of Li_3InBr_6.

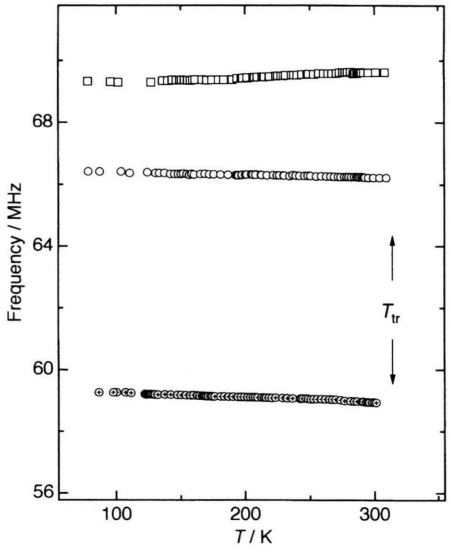

Fig. 2. Temperature dependence of the ^{81}Br NQR frequencies in Li_3InBr_6.

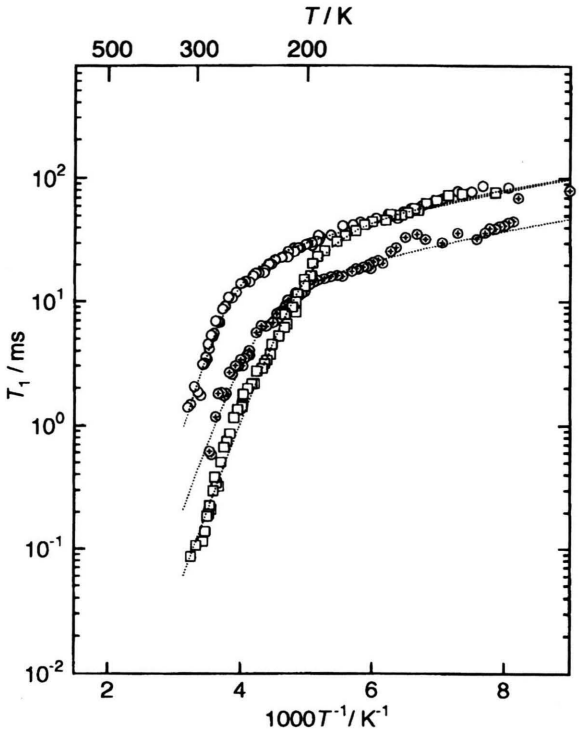

Fig. 3. Temperature dependence of the spin-lattice relaxation times of ^{81}Br NQR in the low-temperature phase of Li_3InBr_6. ⊕: lowest resonance line, ○: middle resonance line, □: highest resonance line.

Table 1. The parameters of (1) for Li_3InBr_6.

NQR line	a	n	b	E_a(kJ/mol)
Highest	8.0×10^{-7}	2	6.1×10^3	29
Middle	8.3×10^{-7}	2	6.3×10^3	36
Lowest	1.7×10^{-7}	2	2.3×10^5	28

dence of the ^{81}Br NQR frequencies. With rising temperature, frequencies of two lines decrease slightly, while that of the third increases. At the phase transition all lines disappeared. Figure 3 shows the temperature dependence of the three spin-lattice relaxation times of ^{81}Br NQR in the low-temperature phase. With rising temperature, the relaxation times decreased because of lattice vibrations. Above about 200 K they decreased exponentially. At the high temperatures, T_1 is in the order highest resonance line < lowest one < middle one. (T_1) is generally expressed by [5]

$$1/T_1 = aT^n + b \exp(-E_a/RT), \quad (1)$$

where E_a is the activation energy of the motion. By fitting (1) to the experimental values, we obtained the parameters listed in Table 1.

The ^{115}In NMR spectrum in the low-temperature phase was very broad and yielded a full width at half magnitude (FWHM) of 7–38 kHz between 485 and 286 K, as shown in Figure 4. These findings suggest that the nuclear quadrupole interaction is rather large. A plot of the FWHM of the ^{115}In NMR spectrum vs. temperature is shown in Figure 5. With increasing temperature, the

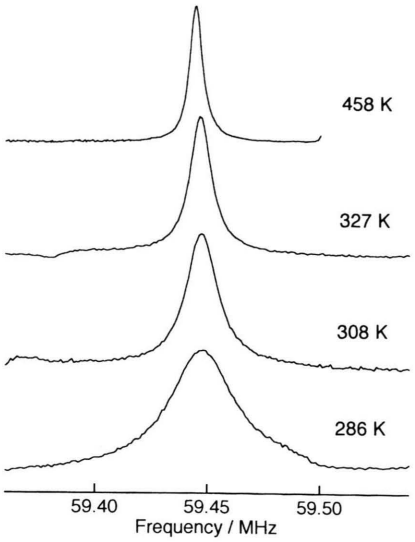

Fig. 4. ^{115}In NMR spectra of Li_3InBr_6 at various temperatures.

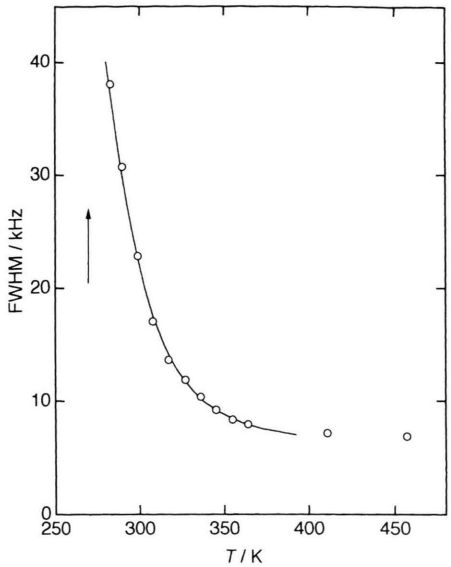

Fig. 5. Plot of the full width at half magnitude (FWHM) of ^{115}In NMR vs. temperature in Li_3InBr_6.

FWHM decreased first abruptly and then gradually. This motional narrowing occurs much above the transition temperature. When the motional narrowing occurs due to the motion of ions in the crystal, the relaxation between the FWHM and the correlation time τ_c of the motion is expressed by [6]

$$\tau_c = (1/\alpha\delta\omega)$$
$$\tan[\pi(\delta\omega^2 - \delta\omega_A^2)/2(\delta\omega_B^2 - \delta\omega_A^2)], \quad (2)$$

where $\delta\omega_B$, $\delta\omega$, and $\delta\omega_A$ are the line widths below, within, and above the motional narrowing, respectively. α is constant and usually unity. From the observed $\delta\omega_B$ $\delta\omega$, and $\delta\omega_A$, and by assuming $\alpha = 1$, τ_c was obtained and plotted against the inverse temperature in Figure 6. Assuming an Arrhenius activation process for τ_c, one has

$$\tau_c = \tau_0 \exp(E_a/RT). \quad (3)$$

From the linear relation between ln τ_c and $1/T$, the activation energy was found to be 26 kJ/mol. After the occurrence of the motional narrowing, the FWHM was 7 kHz. We also calculated the FWHM from the second moment by assuming that the shape of the spectrum is Gaussian. The second moment was evaluated by using the In-Br bond length of 2.76 Å which was obtained by assuming that the crystal structure of Li_3InBr_6 equals that of Li_3InBr_6 [7] and that the main contribution comes from the nearest neighbors. The FWHM thus obtained was 2.2 kHz for Li^+ diffusion. This value is smaller than the observed one, suggesting that the line width is affected

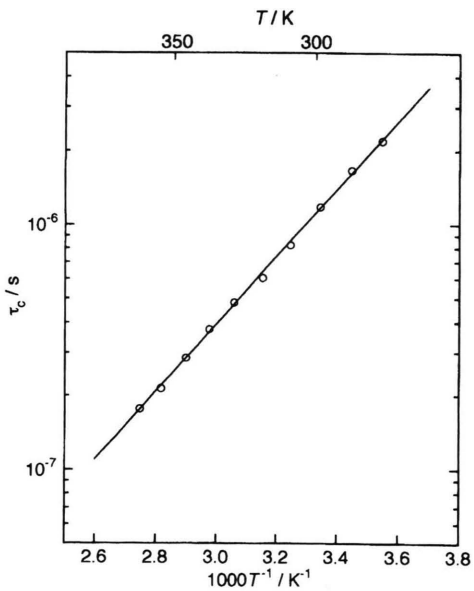

Fig. 6. Plot of the correlation time vs. the inverse temperature in Li_3InBr_6.

by other factors, such as the quadrupole coupling interaction and the aniosotropy of the chemical shift.

Figure 7 shows the ^6Li and ^7Li NMR spectra at various temperatures in Li_3InBr_6. Between 77 and 310 K, the ^7Li NMR spectrum does not change and has a constant

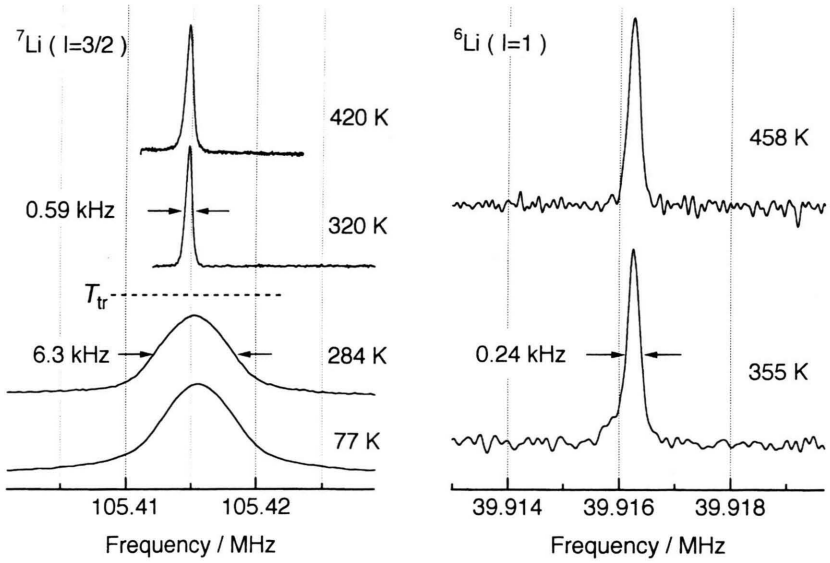

Fig. 7. ^{6}Li and ^{7}Li NMR spectra at various temperatures in Li_3InBr_6.

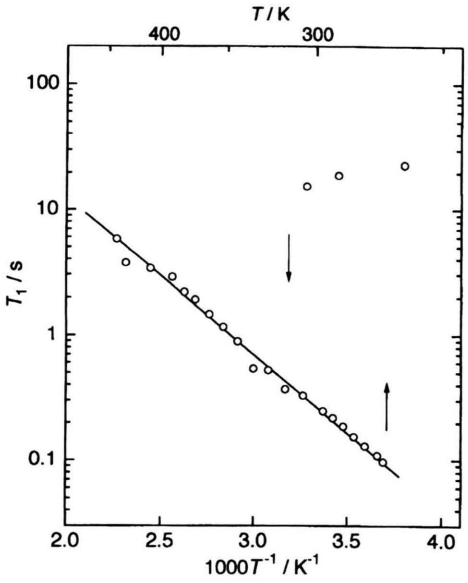

Fig. 8. Temperature dependences of the ^{7}Li NMR spin-lattice relaxation time in Li_3InBr_6. The squares and circles represent the relaxation times in the low and high temperature phases, respectively.

FWHM of 6.3 kHz, indicating that in the low temperature phase diffusion of Li^+ does not occur. Therefore, according to the NQR results, the motion in the low temperature phase is reorientation of the $InBr_6^{3-}$ ion. The FWHM in the high temperature phase was 0.59 kHz for ^{7}Li NMR and 0.24 kHz for ^{6}Li NMR, indicating that diffusion of Li^+ occurs. As the ratio of the former width to the latter one is equal to the ratio of the gyromagnetic ratios of ^{7}Li and ^{6}Li, the line width was found to be determined by dipole-dipole interactions.

Figure 8 shows the temperature dependence of the ^{7}Li NMR spin-lattice relaxation time in Li_3InBr_6. When the temperature rose from 270 K up to near the phase transition point (314 K), the relaxation times were about ten seconds. With further increasing temperature, the relaxation time jumped down at 314 K and then increased gradually. When the temperature fell from about 440 K, the relaxation time decreased linearly. When the temperature reached about 270 K, the relaxation time jumped up to about twenty seconds. On cooling from 440 K, the relaxation time probably changed by rapid motions. Since diffusion of Li^+ occurred in the high temperature phase, the relaxation time is considered to be governed by this motion and is generally expressed by the equation [8]

$$1/T_1 = C^2[\tau_c/(1 + \omega_0^2\tau_c^2) + 4\tau_c/(1 + 4\omega_0^2\tau_c^2)], \quad (4)$$

where C is constant and ω_0 is the resonance frequency. By fitting the above equation and (3) to the observed relaxation times under the condition $1 \gg \omega_0\tau_0$, the activation energy of the diffusion of the Li^+ ion was obtained to be 24 kJ/mol.

Figure 9 reproduces the temperature dependence of the electric conductivity in Li_3InBr_6. The high-temperature phase exhibits a conductivity of more than 10^{-3} S/cm, whereas the low-temperature phase has a

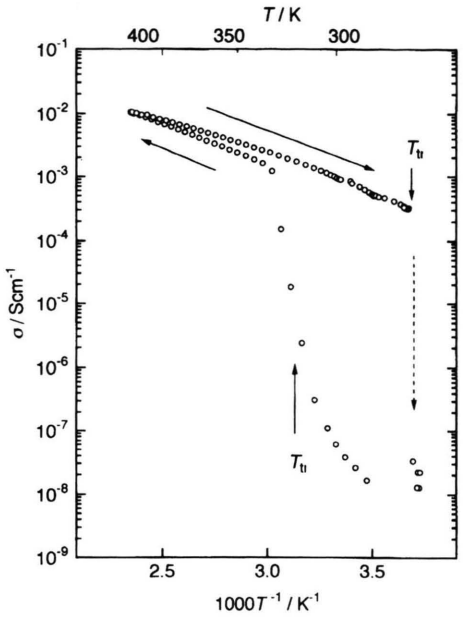

Fig. 9. Temperature dependence of the electric conductivity of Li_3InBr_6.

small conductivity. An abrupt increase in the conductivity was found near the transition temperature, the high-temperature phase being a super ionic conductor where the carrier is Li^+, as mentioned above. The activation energy is obtained from the equation [9]

$$\sigma(T) = \sigma_0 \exp(-E_a/RT), \tag{5}$$

where σ is the electric conductivity. By fitting (5) to the observed data, the activation energy was evaluated to be 25 kJ/mol, which agrees well with the value estimated on the basis of the NMR measurements. This finding indicates that Li^+ contributes the ionic conduction.

$NaInBr_4$

Figure 10 shows the DTA curve for $NaInBr_4$. Two endothermic peaks appeared at 315 and 383 K on heating, while two exothermic ones appeared at 383 and 287 K on cooling. A small hysteresis was observed for the peak at the lower temperature, indicating that this phase transition is of the first order.

$NaInBr_4$ yielded four ^{81}Br NQR lines at 101.180, 110.234, 110.494, and 111.779 MHz at 77 K. This finding indicates the presence of four nonequivalent Br atoms in the crystal and is consistent with the crystal structure reported by Staffel and Meyer [10]. The mean

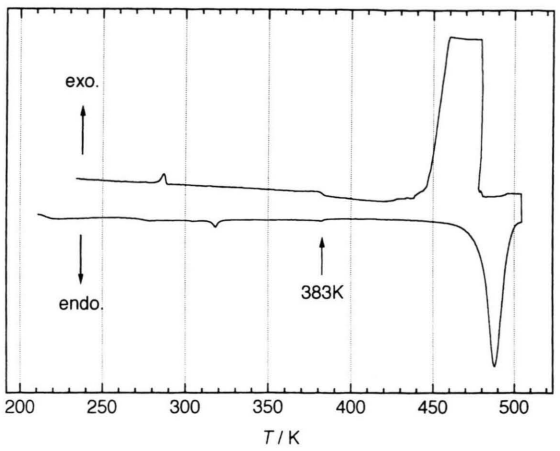

Fig. 10. DTA curve of $NaInBr_4$.

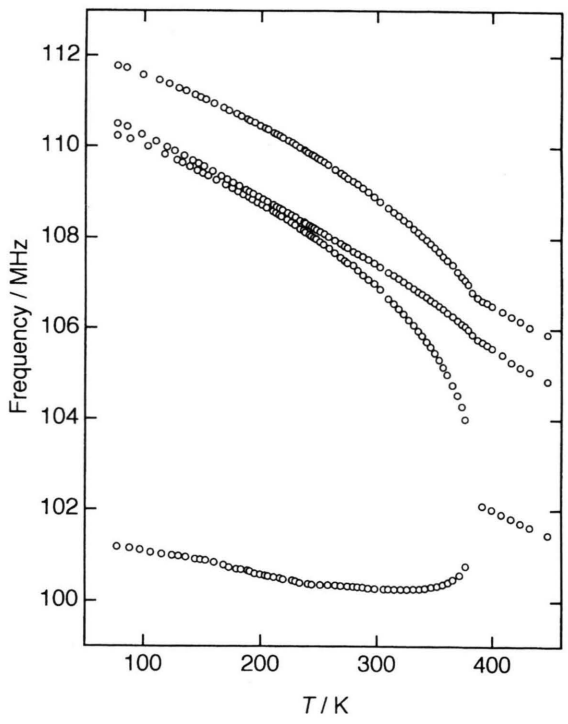

Fig. 11. Temperature dependence of the ^{81}Br NQR frequencies in $NaInBr_4$.

^{81}Br NQR frequency of the $InBr_4^-$ anion in $NaInBr_4$ is 108.422 MHz and is much higher than that (64.971 MHz) of the $InBr_6^{3-}$ anion in Li_3InBr_6, indicating that the ionicity of the In-Br bond is larger in the latter anion than in the former.

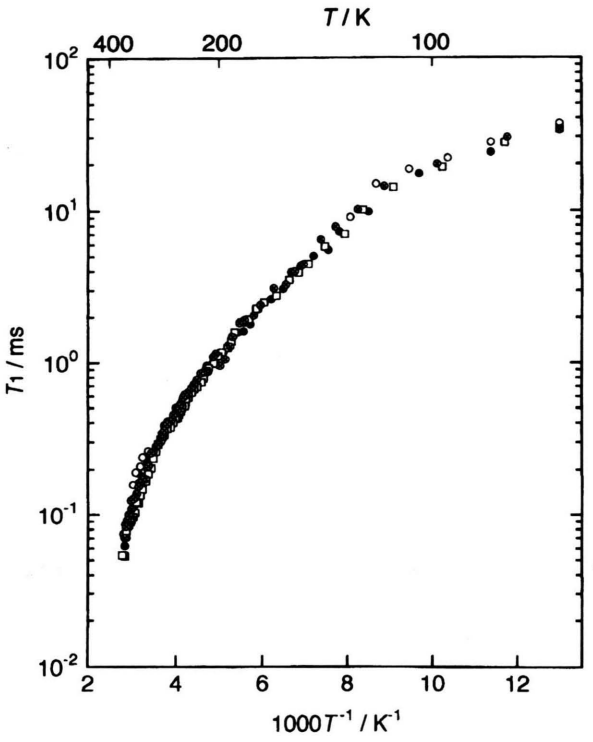

Fig. 12. Temperature dependence of the ^{81}Br NQR spin-lattice relaxation times in $NaInBr_4$. ○ : lowest resonance line, ● : second lowest resonance line, □ : second highest resonance line, ⊕: highest resonance line.

Figure 11 shows the temperature dependence of the ^{81}Br NQR frequencies in $NaInBr_4$. When the temperature reached 380 K on heating from 77 K, the two lower resonance lines coalesced into one line, and the higher ones changed their slopes, suggesting the presence of a second order phase transition, but no anomaly was observed near 315 K, where the peak was observed in the DTA measurements.

Figure 12 shows the temperature dependence of ^{81}Br NQR spin-lattice relaxation times in $NaInBr_4$. The four resonance lines exhibited almost the same curve. The relaxation times decreased gradually with increasing temperature. The decrease in the relaxation time from 77 K up to 110 K showed the T^2 temperature dependence caused by the lattice vibrations. The relaxation times at higher temperatures did not follow the T^2 law, suggesting that the relaxation times did not decrease according to the ionic motion. When the relaxation time is affected by a phase transition, the equation of its temperature dependence has been given by Bonera et al. [11]. By fitting the equation to the experimental data, the following equation was obtained:

$$1/T_1 = 9\{\ln[T_{tr}/(T_{tr} - T)] - 1\}. \quad (6)$$

The observed relaxation times could well be fitted to (6), as shown in Figure 13. Therefore, the relaxation time above 110 K is considered to be influenced by the phase

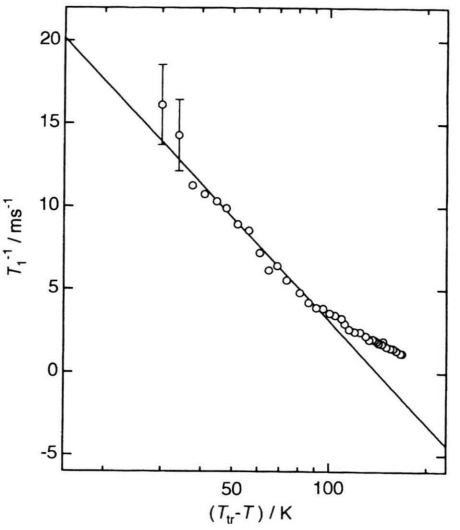

Fig. 13. Plot of ^{81}Br NQR spin-lattice relaxation times vs. $(T_{tr} - T)$ of $NaInBr_4$.

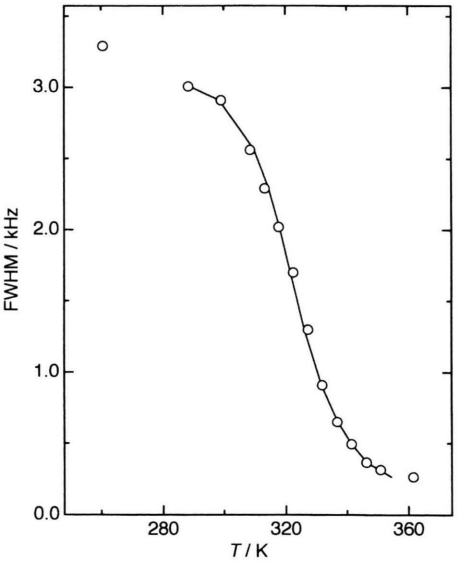

Fig. 14. Temperature dependence of the FWHM of ^{23}Na NMR for $NaInBr_4$.

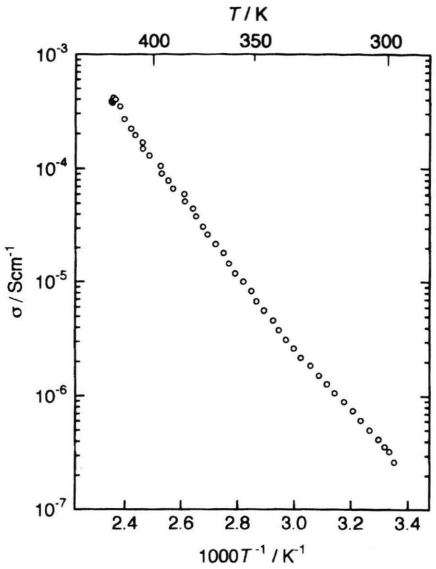

Fig. 15. Temperature dependence of the electric conductivity of $NaInBr_4$.

transition. In the high-temperature phase, the relaxation time was too short ($T_1 < 10^{-4}$s) to be measured.

Figure 14 shows the temperature dependence of the FWHM of the ^{25}Na NMR spectrum in $NaInBr_4$. The FWHM after the motional narrowing was reduced to 0.27 kHz, suggesting that diffusion of Na^+ occurred. By fitting (2) and (3) to these data, the activation energy was evaluated to be 62 kJ/mol. This value is much larger than that of the Li^+ diffusion.

Figure 15 shows the temperature dependence of the electric conductivity of $NaInBr_4$. With increasing temperature, the conductivity increased linearly, but the slope of the curve changed at about 330 K. By fitting (6) to the observed data in the higher temperature range, the activation energy was evaluated to be 64 kJ/mol.

Acknowledgement

This work was supported by the Grant-in-Aid for Scientific Research on Priority Area of "Solid State Ionics", (Area No. 260) from the Ministry of Education, Science and Culture, Japan.

[1] K. Yamada, Y. Tomita, and T. Okuda, J. Mol. Struct. **345**, 219 (1995).
[2] K. Yamada, M. Kinoshita, K. Hosokawa, and T. Okuda, Bull. Chem. Soc. Japan **66**, 1317 (1993).
[3] K. Yamada, K. Isobe, E. Tsuyama, T. Okuda, and Y. Furukawa, Solid State Ionics **79**, 152 (1995).
[4] F. Izumi, The Rietveld Method, Edited by R. A. Young, University Press, Oxford 1993, p. 236.
[5] H. Chihara and N. Nakamura, Advances in Nuclear Quadrupole Resonance, Vol. 4, ed. by J. A. S. Smith, Heyden & Son Ltd., London 1980, p. 37.
[6] A. Abragam, Principles of Nuclear Magnetism, University Press, Oxford 1961, p. 233.
[7] A. Bohnsack, G. Balzer, M. S. Wickleder, H.-U. Gudel, and G. Meyer, Z. Anorg. Allg. Chem. **623**, 1352 (1997).
[8] N. Bloembergen, E. M. Purcell, and R. Pound, Phys. Rev. **73**, 679 (1948).
[9] S. Chandra, Superionic Solid, Principles and Applications, North-Holland Publishing Company, Amsterdam 1981, p. 225.
[10] T. Staffel and G. Meyer, Z. Anorg. Allg. Chem. **574**, 107 (1989).
[11] G. Bonera, F. Borsa, and A. Rigamonti, Phys. Rev. **B2**, 2784 (1970).